

CHEMISTRY

A European Journal

A Journal of



Accepted Article

Title: Cancer-targeting Functionalization of Selenium-Containing Ruthenium Conjugate with Tumor Microenvironment-Responsive Property to Enhance Theranostic Effects

Authors: Zhennan Zhao, Pan Gao, Yuanyuan You, and Tianfeng Chen

This manuscript has been accepted after peer review and appears as an Accepted Article online prior to editing, proofing, and formal publication of the final Version of Record (VoR). This work is currently citable by using the Digital Object Identifier (DOI) given below. The VoR will be published online in Early View as soon as possible and may be different to this Accepted Article as a result of editing. Readers should obtain the VoR from the journal website shown below when it is published to ensure accuracy of information. The authors are responsible for the content of this Accepted Article.

To be cited as: *Chem. Eur. J.* 10.1002/chem.201705561

Link to VoR: <http://dx.doi.org/10.1002/chem.201705561>

Supported by
ACES

WILEY-VCH

Cancer-targeting Functionalization of Selenium-Containing Ruthenium Conjugate with Tumor Microenvironment-Responsive Property to Enhance Theranostic Effects

Zhennan Zhao, Pan Gao, Yuanyuan You and Tianfeng Chen*

Abstract: A multifunctional ruthenium (Ru)-based conjugate **Ru-BSe** was designed and synthesized. The Ru complex with favorable bioimaging function was covalently linked with a cancer-targeted molecule that could be effectively internalized by the tumor to realize enhanced theranostic effects. The pH-response of the Ru conjugate in tumor acidic microenvironment causes ligand substitution and release of therapeutic complex. This activated complex remains inert to the reducing biomolecule-glutathione and terminally locates in mitochondria, where it triggers oxidative stress, and activates intrinsic apoptosis. Real-time monitoring reveals that this Ru conjugate could selectively accumulate in tumor tissue *in vivo*, which significantly suppress tumor progression and alleviate the damage to normal organs, realizing the precise cancer theranosis.

Introduction

Cancer theranosis offers an appealing strategy in cancer treatment by combination of chemotherapy with early and timely diagnosis of tumor carcinogenesis.^[1] Typically, *in vivo* applications of chemotherapeutic agents are hindered by the drawbacks of low bioavailability, lack of selectivity toward tumor and intrinsically non-fluorescence *etc.*^[2] Taking advantages of targeted drug delivery system (DDS), small molecules could be developed as theranostic prodrug that being real-time monitored and selectively delivered to tumors.^[3] The prodrug can be activated by intracellular thiols and changes in pH to realize increased drug bioavailability in the tumor.^[4]

Considering that some transition-metal complexes display favorable phosphorescent properties, it is accessible that metal complexes could be developed as theranostic agents.^[5] Among anticancer metallodrugs, Ruthenium (Ru) complexes are potential alternatives for platinum-based cancer drugs. Currently, the sodium analog of KP1019, i.e., sodium trans-[tetrachlorobis-(1*H*-indazole)ruthenate(III)] {KP-1339/IT139, Na trans-[RuCl₄(Hind)₂] } was selected for clinical trials, while Ru(II) polypyridyl complexes, TLD-1433, entered phase IB clinical trials as a photodynamic therapy agent for with bladder cancer.^[6] Meanwhile, phosphorescent metal complexes with advantageous photophysical features are desirable for biological imaging application. Therefore, by tuning auxiliary ligands, the properties of complexes can be modified to achieve both therapy and diagnosis functions within a single molecule.^[7] Another effective strategy that uses metal complexes containing

anticancer ligands with clear action mechanisms has kindled great interest of chemists. Recently, studies found that complexes, with conjugation of chemotherapeutic agents, display potent inhibitive effects on proliferation of cancer cells.^[8]

The anticancer potency of selenium (Se)-containing compounds has been well-documented in previous studies.^[9] Among these agents, organic selenadiazole derivatives exhibit outstanding anticancer activities,^[10] but their drawbacks, like poor solubility and unsatisfied luminescent properties, limit their theranostic applications *in vivo*. Therefore, studies have been conducted to solve this problem employing metal complexes. Remarkably, Chao et al. have developed phosphorescent Se-containing iridium(III) complexes that are enable for tracking of mitochondrial morphological changes in cells.^[11] Our previous studies showed that the introduction of Se-containing ligand into Ru complexes effectively enhanced the apoptosis-inducing activity against cancer cells, and targeted DDS was capable to enhance the selectivity of metal complexes towards cancer cells.^[12] Therefore, the introduction of Se into luminescent metal complexes and the further cancer targeting design may be a potent strategy for discovery of theranostic agents for precise cancer treatment.

Bearing these facts in mind, in the study, we have designed and synthesized a Se-containing Ru conjugate covalently linked with a cancer-targeted molecule (**Ru-BSe**, **Scheme 1a**) that could selectively accumulate in cancer cells during circulation *in vivo* to realize enhanced theranostic effects and alleviate the systemic toxicity of metal complexes. The phosphorescent emission property of Ru(II) conjugates allows the real-time tracking and imaging of the drug inside the biological systems. By utilizing the cancer targeting design, biotinylated **Ru-BSe** can be selectively internalized by tumor cells, thus minimizing side effects towards normal organs in tumor-bearing xenograft mice.

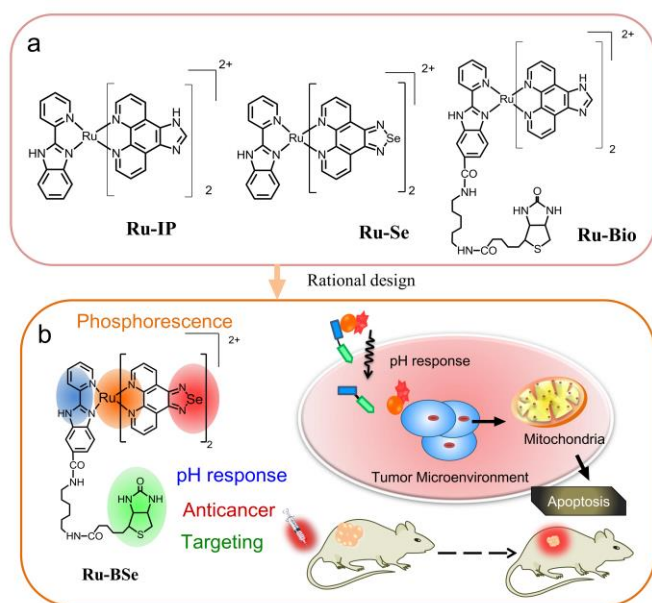
Results and Discussion

Rational design and tumor microenvironment responsive property of Ru-BSe

In this study, a series of Ru complexes with various structures were designed and synthesized to examine the effects of Se substitution and targeted modification on the activity of complex (**Scheme 1**). The synthetic procedures of Ru(II) complexes were illustrated in **Figure S1** and the chemical structures were characterized by ESI-TOFMS analysis, CHN elemental analysis, ¹H and ¹³C NMR spectroscopy (**Figure S2-S16**). The photophysical data (**Table S1**, **Figure S17**) show that Ru(II) complexes possess red phosphorescence ($\lambda_{em} \approx 600$ nm)

[a] Z. Zhao, P. Gao, Y. You, Prof. T Chen
Department of Chemistry
Jinan University, Guangzhou 510632 (P. R. China)
E-mail: tchentf@jnu.edu.cn

Supporting information for this article is given via a link at the end of the document.



Scheme 1. Rational design and theranostic function of Ru(II) conjugate. (a) Chemical structures of Ru(II) compounds in this work. (b) The cancer targeted selenium-containing conjugate **Ru-BSe** is capable for tumor diagnosis and therapy.

with long emission lifetime ($\tau_{em}=0.42\sim0.64\ \mu s$), which allows the real-time tracking and imaging of drug in the biological systems.

The protonation/deprotonation processes can perturb the electronic properties of the molecules, especially metal complexes,^[5b, 13] which can result in the change on coordination ability of the ligand. Therefore, we examined the effect of the protonation/deprotonation of the imidazole ring within the Bioben ligand on the stability of Ru(II) conjugate in Na_2HPO_4 /citric acid buffer.^[14] When the pH was changed from weakly basic (8.5) to acidic (3.1), **Ru-BSe** experienced spectral changes, including increased ligand absorption band (290–350 nm), declining metal-to-ligand charge transfer (¹MLCT) absorption band (400–530 nm) and decreased emission (³MLCT excited state) (**Figure S18**). Additionally, we also found time-dependent changes in the spectrum of **Ru-BSe** after incubation in aqueous solution at pH=6.86 (**Figure 1a-b**). Such a weakly acidic condition simulates the environments of solid tumors and hypoxia tissues, which indicates the tumor microenvironment-responsive property of the Ru conjugate.^[15] This hypothesis was further verified by ESI-TOFMS analysis, demonstrating these changes were attributed to the decomposition of **Ru-BSe** in aqueous solution. Specifically, the peak of $[Ru(phenSe)_2(H_2O)_2]^+$ was detected (**Figure 1c**), suggesting ligand Bioben could be released from **Ru-BSe** (**Figure S19**). Additionally, unlike Pt or Au complexes^[16], the aqueous product $[Ru(phenSe)_2(H_2O)_2]^+$ remained stable in the presence of glutathione (GSH), as no distinct peak ascribed for the adduct of **Ru-BSe** and GSH was detected after 6 and 72-h incubation (**Figure 2a**). GSH is a major antioxidant with detoxifying properties inside cancer cells^[17], preventing cell damage from the exposure of heavy metals. Further examination showed that the pH-responsive release of **Ru-BSe**

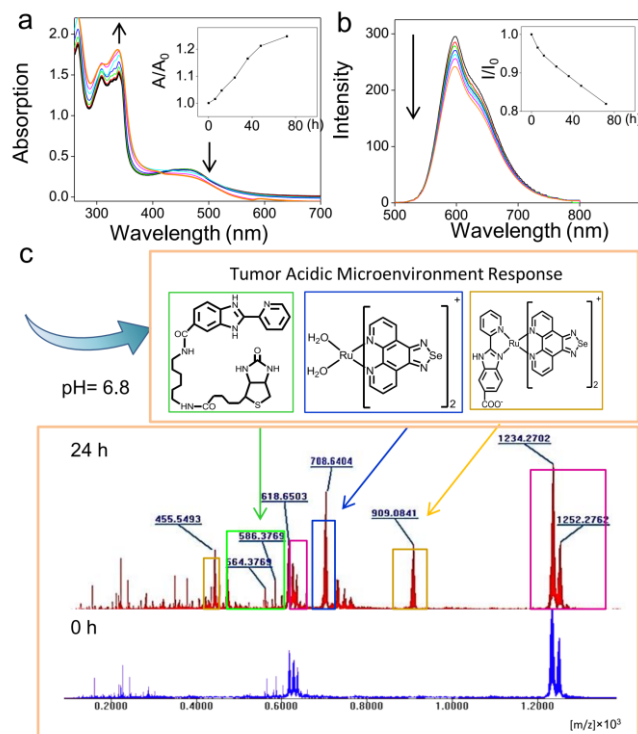
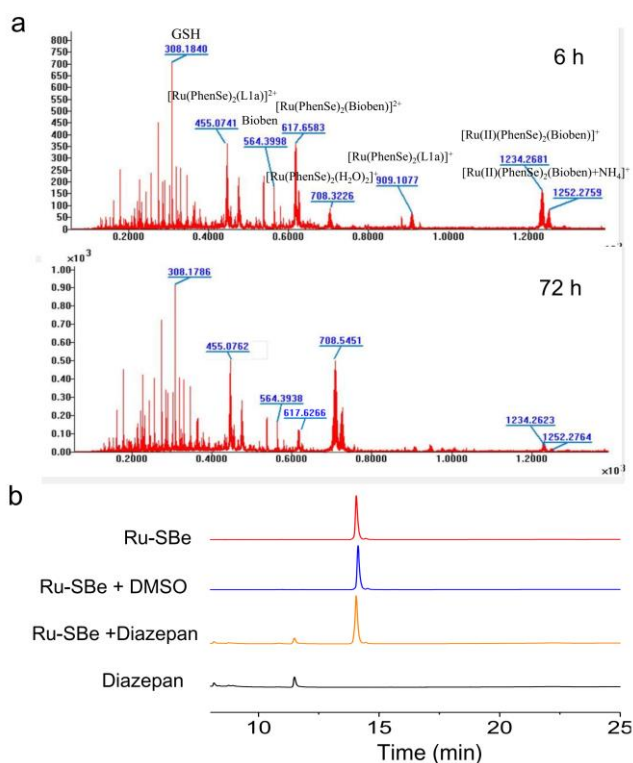


Figure 1. Biological response of Ru(II) conjugate in weakly acidic environment. (a) UV/Vis spectrum and (b) the emission spectrum of **Ru-BSe** in PBS solution (pH=6.86, containing 5% DMSO) after incubation at different time point. *Inset*: Plot of relative absorption (A/A_0 , at 340 nm)/emission intensity (I/I_0 , at 600 nm) versus the incubation time. A_0 and I_0 represent the absorption and emission intensity at 0 h, respectively. (c) The decomposition of **Ru-BSe** in MeOH/Milli-Q H₂O solution (3:7, v:v, containing 10 mM NH_4HCO_3 , pH=6.86) after 24-h incubation before recording by ESI-TOFMS.

was temperature dependent (**Figure S20**). On the other hand, **Ru-BSe** kept stable in DMSO and human plasma solution (**Figure 2b**), implying the significance of weakly environment on the activation of **Ru-BSe** conjugate. Taken together, these results indicate the significance of weakly acidic environment on the decomposition of the conjugate, which could promote the release of therapeutic complex, thus minimize the effect of covalent cancer-targeted unit on the anticancer activity of the prodrug.

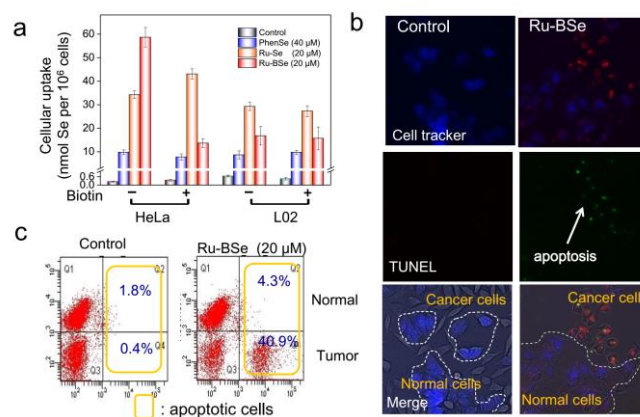
Selective recognition of cancer cells by Ru-BSe to realize tumor diagnosis in vivo

As expected, the formation of Se-containing Ru(II) complexes enhances the solubility of selenadiazole derivatives, resulting in significant influence of cellular uptake (**Figure 3a**). To verify our hypothesis of the cancer-targeted potency of **Ru-BSe**, biotin receptor-positive cancer cells (HeLa) and biotin receptor-negative normal cells (L02)^[18] were incubated with Ru(II) conjugate. We found targeted **Ru-BSe** was preferentially taken up by HeLa cancer cells (**Figure 3a** and **S21**). Moreover, the pretreatment of cells with excess biotin partially blocked the uptake of biotinylated **Ru-BSe**. Furthermore, we employed a co-culture model of HeLa and L02 cells to investigate the selective



induction of apoptosis by Ru-BSe in cancer cells using TUNEL assay. As shown in Figure 3b, formation of DNA fragmentation was detected in most HeLa cells (24 h), which was hardly found in L02 cells. The ratio of apoptotic HeLa cells in the co-culture population was increased to 20.8% after the treatment of Ru-BSe, which was higher than that of L02 cells (at 2.1%) (Figure 3c). Moreover, the addition of endocytosis inhibitor influenced the cellular uptake of the complexes in different degree (Figure S22), indicating the important contribution of receptor-mediated endocytotic (energy-dependent) pathway to the uptake of Ru-BSe.

In vivo examination was also performed in HeLa-inoculated xenograft mice to investigate the cancer targeting ability of Ru(II) complexes. As reflected by the fluorescent signals of Ru(II) complexes (Figure 4a), Ru-BSe exhibited much higher accumulating efficacy in tumor site within 72-h intravenous injection, than that of Ru-Se. *Ex vivo* imaging can clearly display the biodistribution of Ru(II) complexes in the main organs. The results showed that Ru-BSe was selectively internalized by tumors rather than other organs, while Ru-Se preferentially

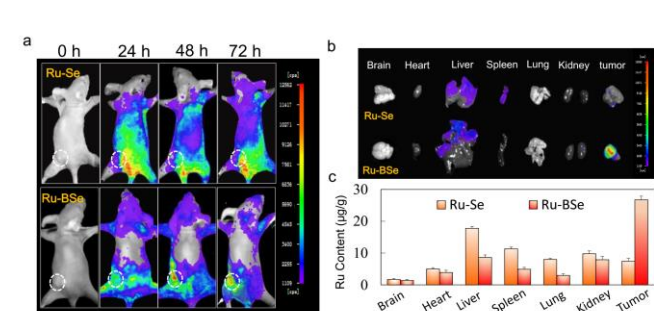


accumulated in liver and spleen (Figure 4b). The biodistribution of Ru(II) complexes was further verified by determining Ru content in organs after 30 days treatment. The Ru content in Ru-BSe-treated tumor was significantly higher than that of normal tissues, and approximately 3 times of Ru-Se group (Figure 4c).

Activation of mitochondrial dysfunction by Ru-BSe induced intrinsic apoptosis

Consistent with our previous studies, Se substitution significantly enhanced the anticancer efficacy of Ru(II) complexes (Table 1).^[12a] Firstly, we demonstrated that, the therapeutic metallodrug [Ru(phenSe)₂Cl₂] and its aquation product [Ru(phenSe)₂Cl₂](aq) both exhibit potent anticancer activities,

induced apoptosis by Ru-BSe in cancer cells using TUNEL assay. As shown in Figure 3b, formation of DNA fragmentation was detected in most HeLa cells (24 h), which was hardly found in L02 cells. The ratio of apoptotic HeLa cells in the co-culture population was increased to 20.8% after the treatment of Ru-BSe, which was higher than that of L02 cells (at 2.1%) (Figure 3c). Moreover, the addition of endocytosis inhibitor influenced the cellular uptake of the complexes in different degree (Figure S22), indicating the important contribution of receptor-mediated endocytotic (energy-dependent) pathway to the uptake of Ru-BSe.



induced apoptosis by Ru-BSe in cancer cells using TUNEL assay. As shown in Figure 3b, formation of DNA fragmentation was detected in most HeLa cells (24 h), which was hardly found in L02 cells. The ratio of apoptotic HeLa cells in the co-culture population was increased to 20.8% after the treatment of Ru-BSe, which was higher than that of L02 cells (at 2.1%) (Figure 3c). Moreover, the addition of endocytosis inhibitor influenced the cellular uptake of the complexes in different degree (Figure S22), indicating the important contribution of receptor-mediated endocytotic (energy-dependent) pathway to the uptake of Ru-BSe.

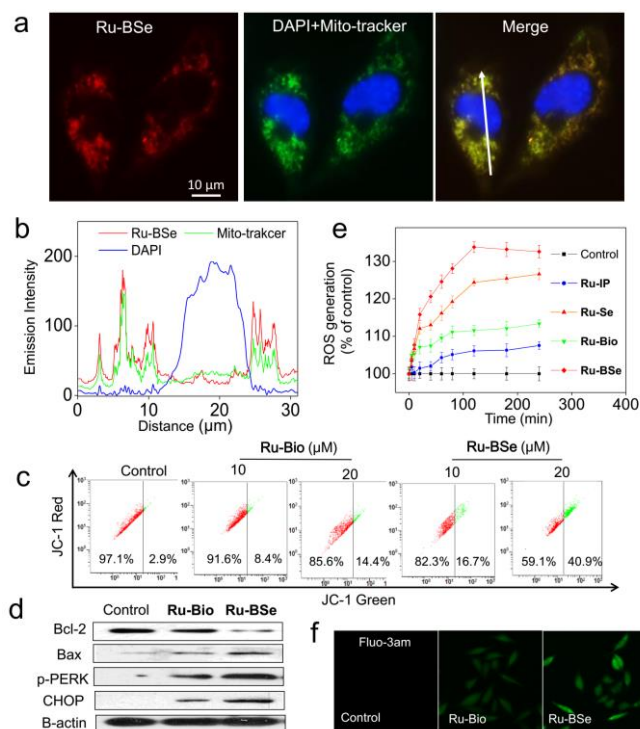


Figure 5. Ru-BSe triggers mitochondria dysfunction and ER stress in HeLa cells. (a) Fluorescent image and (b) emission intensity analysis of **Ru-BSe** (20 μM) and Mito-tracker after incubation for 6 h. Cells were visualized in the green channel for Mito-tracker ($\lambda_{\text{ex}}=488$ nm, $\lambda_{\text{em}}=500\text{--}560$ nm) and red channel for Ru complex ($\lambda_{\text{ex}}=500$ nm, $\lambda_{\text{em}}=600\text{--}650$ nm), respectively. (c) Change of mitochondrial membrane potential examined by JC-1. (f) Western blot analysis for expression levels of Bcl-2 family members and ER stress related proteins that regulated by treatment of Ru conjugates (20 μM) for 72 h. (e) Induction of ROS generation by Ru(II) complexes (20 μM) in 4 h. (f) Cytoplasmic calcium ion level in HeLa cells exposed to 20 μM Ru conjugates (30 min).

but they showed low selectivity between cancer and normal cells (Table S2). After targeting functionalization, **Ru-BSe** demonstrated a broad range of anticancer action towards cancer cell lines. Especially, **Ru-BSe** displayed favorable tumor inhibitory effects toward HeLa cells with IC_{50} value of 15.3 μM , which was competitive with that of cisplatin (16.5 μM). Despite this potency, the prodrug **Ru-BSe** showed higher selectivity against cancer cells compared with cisplatin and **Ru-Se** (without target unit). Studies have proven that the anticancer actions of drugs are associated to their intracellular localization of anticancer drugs.^[19] Previously, we found that the cellular localization of iron(II) polypyridyl complexes determines their anticancer action mechanisms.^[20] Cytosolic Iron(II) complexes exhibited anticancer and antiangiogenic potencies by targeting mitochondria to trigger cancer cell apoptosis.^[21] Therefore, in this study, we next set out to elucidate the relationship between the anticancer action mechanisms and cellular localization of **Ru-BSe**. **Ru-BSe** accumulated in the cytoplasm after incubation for 6 h. The notable merge of mitochondria (green) and the conjugate (red) was observed (Figure 5a), with Pearson's colocalization coefficient at 0.90. Meanwhile, quantification of the luminescence intensity further confirmed the overlap of

Table 1. Cytotoxicity of Ru(II) complexes on cancer and normal cell lines.

Complex	IC_{50} (μM)							SI*
	HeLa	A549	MCF-7	MDA-MB-231	HepG2	L02	NCM460	
Ru-IP	67.8	104.3	52.7	50.2	57.8	88.4	95.3	1.30
Ru-Se	21.0	19.4	21.2	18.4	17.8	20.3	25.4	0.97
Ru-Bio	44.7	58.6	87.5	57.4	51.8	126.3	112.6	2.83
Ru-BSe	15.3	17.4	21.0	22.7	34.1	77.6	68.5	4.24
Cisplatin	16.5	16.9	15.7	21.7	13.6	7.3	9.4	0.46

*SI (Safe Index) = $\text{IC}_{50}(\text{L02})/\text{IC}_{50}(\text{HeLa})$, which reflects the side effect of complexes.

mitochondria and **Ru-BSe** (Figure 5b). Therefore, we also examined the effect of **Ru-BSe** on the mitochondrial membrane potential ($\Delta\psi\text{m}$) by JC-1 flow cytometric analysis. **Ru-BSe** significantly induced dose-dependent disruption of $\Delta\psi\text{m}$ in HeLa cells, as reflected by the shift of JC-1 fluorescence from red to green in cells (Figure 5c). In contrast, only slight change in $\Delta\psi\text{m}$ of cells was observed in cells exposed to **Ru-Bio**. The loss of $\Delta\psi\text{m}$ in cells caused by the mitochondrial dysfunction is closely connected with the regulation by Bcl-2 family proteins.^[22] Our results showed that **Ru-BSe** dramatically suppressed the expression of Bcl-2 (anti-apoptotic proteins) and upregulated the expression of Bax (pro-apoptotic proteins) in HeLa cells (Figure 5d). The mitochondrial respiratory chain is a potential source of ROS, thus the observation of **Ru-BSe**-induced mitochondrial dysfunction encouraged us to examine intracellular levels of reactive oxygen species (ROS).^[23] Treatments of Se-containing complexes **Ru-Se** and **Ru-BSe** significantly triggered excessive generation of ROS in cells within 4 h, while the complexes without Se induced much lower ROS generation (Figure 5e). The accumulation of excessive ROS generation triggers endoplasmic reticulum (ER) stress, promoting apoptosis in cancer cells.^[24] The increased expression level of ER stress related proteins (p-PERK and CHOP) verified elevated ER stress level in HeLa cells after the treatment of Se-containing

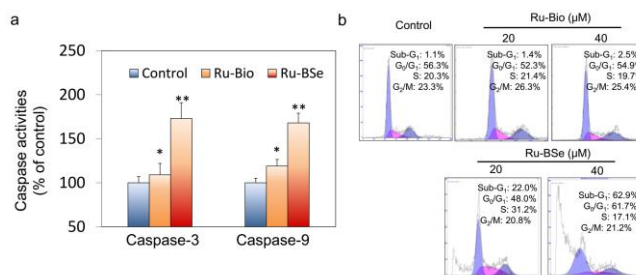


Figure 6. Se-containing Ru(II) conjugates induced apoptosis in HeLa cells. (a) Treatment of Ru(II) conjugates activated caspase3/9 activity in HeLa cells, which was determined by synthetic fluorescent substrates. (b) After treatment of Ru(II) conjugates for 72 h, apoptotic cell death was examined by flow cytometric analysis.

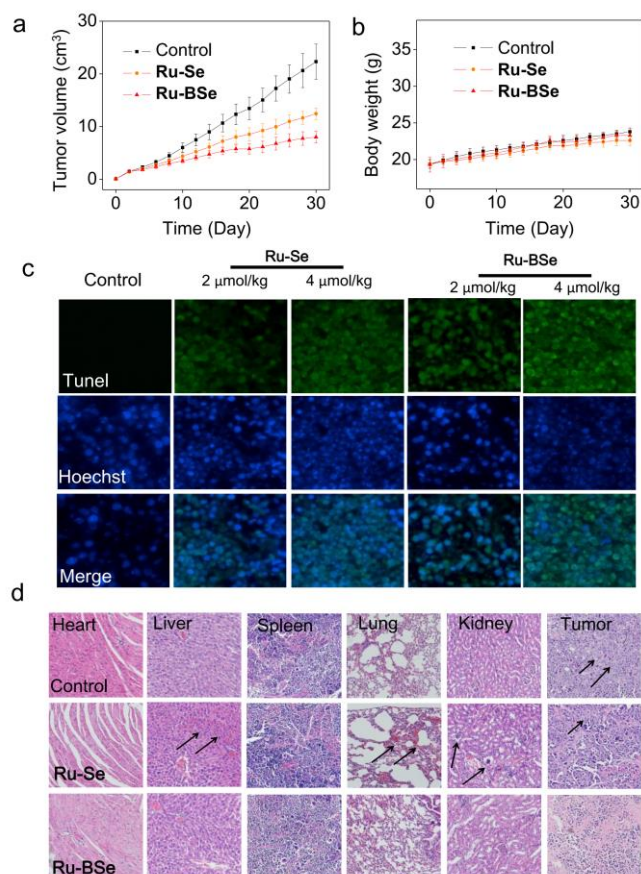


Figure 7. Targeted Ru-BSe conjugate nullifies systemic toxicity in HeLa xenograft mice *in vivo*. (a, b) The change in tumor volume and body weight (dose, 4 $\mu\text{mol/kg}$, every 2 days). (c) TUNEL staining analysis of tumor cell apoptosis. (d) The toxicity of Ru(II) complexes on major organs after 30-day treatment (a dose of 4 $\mu\text{mol/kg}$ every 2 days). The arrows highlight the site with pathological change.

complex. The release of stored calcium in ER is a sensitive indicator of ER stress,^[25] so we tested the calcium ion levels in cytoplasm by using the calcium fluorescence probe Fluo-3AM. A large elevation in the cytoplasmic Ca^{2+} was detectable in cells exposed to 20 μM **Ru-BSe** for 30 min, indicating the ROS-mediated ER stress was activated (**Figure 5f**). A rise in cytoplasmic Ca^{2+} contributed to the rapid increase of cation in mitochondria, which would further promote the bioenergetics failure of the organelle, leading the activation of intrinsic apoptosis pathways and caspases proteins. Correspondingly, we also found the treatment of Se-containing Ru(II) complex contributed to the activation of caspase-3 and 9 (**Figure 6a**), which are well-known as the important mediators of intrinsic apoptosis. Finally, propidium iodide (PI)-flow cytometric analysis was performed to examine the induction of apoptosis in cancer by Ru(II) complexes. As reflected by the Sub-G1 cell population (**Figure 6b**), exposure of HeLa cells to **Ru-BSe** (40 μM) for 72 h resulted in an increased percentage of apoptotic cells from 1.1% to 62.9%. Taken together, the introduction of Se(IV) species into Ru(II) complexes effectively triggered mitochondrial dysfunction by regulation of Bcl-2 family proteins, thus leading activation of intrinsic apoptosis via ROS-mediated ER stress signal pathway.

Targeted delivery of Ru-BSe enhanced anti-tumor efficacy and alleviated systemic toxicity

Finally, the *in vivo* antitumor activity and systemic toxicity of **Ru-BSe** were evaluated by using HeLa-inoculated xenograft mice. After the treatment with the complexes for 30 days, the tumor inhibition rates were 44.3% for **Ru-Se** and 64.2% for **Ru-BSe**, respectively (**Figure 7a**). Additionally, no death or obvious change in body weight of mice was observed at this dosage (**Figure 7b**). Moreover, the results of TUNEL staining assay illustrated that Se-containing complexes induced tumor cells

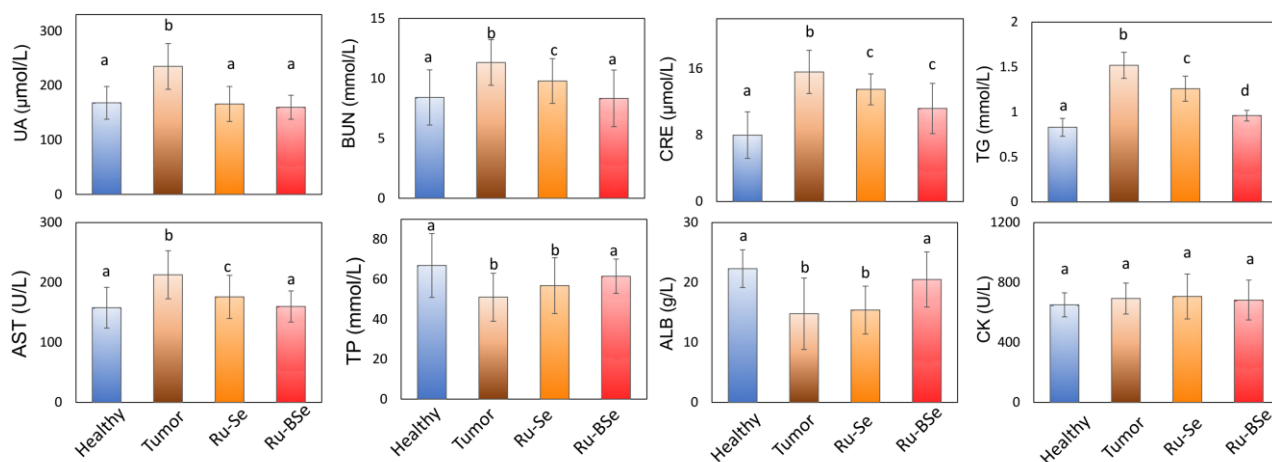


Figure 8. Hematological analysis of healthy and tumor-bearing nude mice, and those treated with Ru-Se or Ru-BSe (4 $\mu\text{mol/kg}$) for 30 days. The nude mice in healthy and tumor-bearing groups were treated with saline. The tested biochemical indexes included uric acid (UA), blood urea nitrogen (BUN), creatinine (CRE), triglyceride (TG), aminotransferase (AST), total protein (TP), albumin (ALB) and creatine kinase (CK).

apoptosis in a dose-dependent manner *in vivo* (Figure 7c). To evaluate the toxic side effects of the complexes *in vivo*, we examined the pathological changes of the tissues by utilizing H&E staining. The targeted complex was capable to deliver Ru-BSe to tumor, thus reducing the toxic effects on liver, lung and kidney (Figure 7d). The hematological analysis was performed to test the effects of Ru(II) complexes on the liver and kidney functions of the treated nude mice. These results reveal that, formation of HeLa xenografts induces damage to the liver and renal function of nude mice, as reflected by the change of values of blood biochemical analysis. For instance, treatment of Ru-BSe (4 $\mu\text{mol/kg}$) effectively alleviated the blood parameters to normal levels, including blood urea nitrogen (BUN), albumin (ALB) uric acid (UA), creatinine (CRE), triglyceride (TG), aminotransferase (AST), total protein (TP) (Figure 8). Collectively, all these data demonstrate that, targeted Ru-BSe could specifically accumulate in the tumor site, thus enhancing antitumor potency and minimizing the undesirable toxic side effects.

Conclusions

We have demonstrated the rational design of Se-containing conjugate Ru-BSe and its application as a potential theranostic agent for precise tumor diagnosis and therapy. The protonation process accelerates the decomposition of Ru-BSe, which promotes release of therapeutic complex from the DDS. The activated product remains inert to GSH and possesses high specificity to mitochondria, where it activates the overproduction of ROS, resulting in intrinsic apoptosis in cancer cells through the induction of endoplasmic reticulum stress signal pathway. The *in vivo* xenograft mice model demonstrates that Ru-BSe possesses enhanced theranostic effects for cancer treatment and reduced systemic toxicity. Such all-in-one theranostic strategy provides a new approach for the rational design of phosphorescent metal complexes that are competent for precise tumor diagnosis and therapy.

Experimental Section

Materials and general instruments: Ruthenium chloride hydrate, cisplatin, metabolic inhibitors, endocytosis inhibitors, 2',7'-dichlorofluorescein diacetate (H₂DCF-DA) and Fluo3-AM solution (1 mM in DMSO, $\geq 99.0\%$) were obtained from Sigma-Aldrich. The TUNEL assay kit was purchased from Roche Applied Science. Other chemical agents from commercial sources were used as received without further purification, including 1-Ethyl-3-(3-dimethylaminopropyl)carbodiimide hydrochloride (EDCI), N-Hydroxysuccinimide (NHS), dichloromethane (DCM), and N,N-Dimethylformamide (DMF). Stock solutions of cisplatin (3 mM) were prepared in saline, while Ru complexes (5 mM) were dissolved in DMSO. All stock solutions were stored at -20°C , thawed and diluted with culture medium prior to each experiment. The ¹H and ¹³C NMR

spectrum of samples in DMSO-d₆ solution were recorded on Bruker AVANCE AV 500 NMR spectrometer, with TMS used as an internal reference. A HORIBA Fluorolog system was employed for emission lifetime measurements. Luminescent quantum yields of complexes were measured with degassed [Ru(bpy)₃](ClO₄)₂ in acetonitrile ($\phi_f=0.062$) as reference. Fluorescent images of cells were recorded on EVOS FL auto microscope (Life Technologies). All animal experiments were performed under the supervision of the Animal Experimentation Ethics Committee of Jinan University.

Synthesis of L1: The ligand L1 was prepared as previously described by Schiffmann et al.^[26]

Synthesis of L1a: 3,4-diaminobenzoic acid (4.56 g, 30 mmol) and copper acetate (5.50 g, 30 mmol) were mixed in 100 mL ethanol/water (1:1, v:v) solution, and then pyridine-2-carbaldehyde (2.68 g, 25 mmol) was added in the solution drop by drop. A dark brown precipitate was formed and continually heated at 80°C for 2 h, then filtered off and suspended in 100 mL of ethanol. To decompose the complex, Na₂S·9H₂O (7.20 g, 30 mmol) was added in the mixture and black precipitate of the formed copper complex was filtered off. The filtrates were concentrated and acidified with HCl in order to help H₂S removing from the solution by heating on the water bath. The raw produce was purified by alumina column chromatography with ethyl acetate/methanol (1:1) solution as eluents. Yield: 79.1%, ¹H NMR (DMSO-d₆, δ ppm): 13.1 (N-H, s, 1H), 8.73 (d, 1H), 8.34 (d, 1H), 8.19 (s, 1H), 7.54 (t, 1H), 7.87 (d, 1H), 7.52 (d, 2H).

Synthesis of compound 2: Compound 2 was synthesized according to previous methods.^[27]

Synthesis of Bioben: Compound L1a (0.49 g, 2.0 mmol) was dissolved in 20 mL dry DMF in 50 mL round-bottom flask under argon atmosphere. EDCI (0.48 g, 2.5 mmol) and NHS (0.27 g, 2.3 mmol) were added in the solution and the mixture was stirred at room temperature for 2 h. Then compound 2 (0.68 g, 2.0 mmol) and 1 mL triethylamine (TEA) were added in the solution and stirred it for another 2 h. After the reaction was completed, a dark yellow precipitate was obtained after the solution was poured into the ice water. The product was filtered off and dried, then purified by silica gel column chromatography using MeOH/DCM (1:1) as eluents to afford compound Bioben as yellow solid. Yield: 42.9%. Anal. Calcd for C₂₉H₃₇N₇O₃S(%): C, 61.79; H, 6.62; N, 17.39. Found (%): C, 61.80; H, 6.59; N, 17.30. ESI-TOFMS (CH₃OH): m/z 586.6404 [M+Na]⁺, 1150.2517 [2M+Na]⁺, ¹H NMR: (DMSO-d₆, δ ppm): 13.33 (d, 1H), 8.77 (d, 1H), 8.51 (d, 1H), 8.35 (d, 1H), 8.27 (s, 1H), 8.03 (m, 1H), 7.83 (t, 1H), 7.74 (q, 1H), 7.56 (t, 1H), 6.40 (d, 2H), 4.29 (t, 1H), 4.13 (t, 1H), 3.29 (q, 2H), 3.09 (q, 1H), 3.04 (q, 2H), 2.80 (dd, 1H), 2.57 (d, 1H), 2.08 (t, 2H), 1.65-1.40 (m, 9H), 1.40-1.20 (m, 6H). ¹³C NMR: (DMSO-d₆, δ ppm): 172.33, 166.97, 163.19, 149.95, 148.64, 142.99, 138.13, 136.60, 134.11, 133.64, 127.78, 125.51, 122.16, 119.00, 110.82, 61.52, 59.66, 55.91, 38.78, 35.70, 29.67, 29.64, 28.69, 28.52, 26.73, 26.65, 25.82.

Synthesis of PhenSe^[12a]: PhenSe([1,2,5]selenadiazolo[3,4-f][1,10]phenanthroline) was prepared based on the previous method. In brief, a mixture of SeO₂ (0.57 g, 0.5 mmol) and 5,6-diamino-1,10-phenanthroline (1.05 g, 0.5 mmol) was dissolved in 200 mL ethanol to reflux for 6 h. Then the solvent was concentrated and washed with 50 mL ethanol. The raw product was recrystallized by methanol and filtered. The pink solid was obtained with a yield of 67.8%.

cis-[Ru(II) (L)₂Cl₂]: The cis-[Ru(II) (L)₂Cl₂] (L= IP or PhenSe, IP= 1H-imidazo[4,5-f][1,10]phenanthroline) was prepared as following: RuCl₃·3H₂O (1 mmol, 0.27 g) and L (2 mmol, 0.44 g for IP or 0.57 g for PhenSe) were mixed in 10 mL of DMF at 140 °C for 6 h under argon atmosphere. After reaction was completed, the solution was cooled to ambient temperature and dissolved in 100 mL cold acetone, and then the formed precipitate was filtered and washed with acetone and diethyl ether. ^[28] Yield: 47.6% for cis-[Ru(II) (IP)₂Cl₂] and 59.3% for cis-[Ru(II) (PhenSe)₂Cl₂].

Synthetic procedure for the complexes: Ligand L1 or Bioben (1 equiv) and the appropriate cis-[Ru(II)(L)₂Cl₂] (1 equiv) were suspended in deoxygenated solution (2-methoxyethanol: H₂O=3:1) and refluxed for 6 h under argon atmosphere in dark. The precipitate was obtained by addition of a saturated aqueous NaClO₄ solution, then filtered off and dried *in vacuo*. The raw products were purified by alumina column chromatography, gradually changing the eluents (DCM /MeOH) from 40:1 to 10:1.

[Ru(II)(IP)₂(L1)](ClO₄)₂ (Ru-IP): Complex Ru-IP was obtained as an orange powder. Yield: 53.6%. Anal. Calcd for C₃₈H₂₅Cl₂N₁₁O₈Ru (%) : C, 48.78; H, 2.69; N, 16.47. Found (%): C, 48.68; H, 2.66; N, 16.39. ESI-TOFMS (CH₃OH): m/z 736.5047 [M-2ClO₄-H]⁺, 368.8029 [M-2ClO₄]²⁺. ¹H NMR (DMSO-d₆, δ ppm): 9.03 (d, 2H), 9.01 (d, 2H), 8.94 (d, 1H), 8.75 (s, 2H), 8.94 (d, 2H), 8.75 (s, 2H), 8.73 (s, 1H), 8.71 (s, 1H), 8.06-8.04 (dd, 4H), 7.95 (s, 4H), 7.79-7.77 (q, 4H). ¹³C NMR (DMSO-d₆, δ ppm): 173.35, 159.72, 155.79, 151.17, 150.37, 149.94, 149.51, 149.45, 147.83, 146.85, 146.54, 146.34, 146.08, 145.70, 144.88, 144.65, 137.62, 129.49, 129.37, 129.04, 126.29, 126.18, 126.12, 125.65, 125.02, 124.66, 124.44, 124.17, 124.07, 121.92, 121.11, 120.31, 119.59, and 112.90.

[Ru(II)(PhenSe)₂(L1)](ClO₄)₂ (Ru-Se): Complex Ru-Se was obtained as a red powder. Yield: 43.7%. Anal. Calcd for C₃₆H₂₁Cl₂N₁₁O₈RuSe₂ (%) : C, 40.58; H, 1.99; N, 14.46; Found (%): C, 40.46; H, 2.05; N, 14.27. ESI-TOFMS (CH₃OH): m/z 866.4620 [M-2ClO₄-H]⁺, 433.8093 [M-2ClO₄]²⁺. ¹H NMR (DMSO-d₆, δ ppm): 9.00 (m, 4H), 8.42 (t, 2H), 8.32 (d, 1H), 8.24 (d, 1H), 8.01 (t, 1H), 7.93 (m, 3H), 7.81 (q, 1H), 7.77 (q, 1H), 7.65 (d, 1H), 7.55 (d, 1H), 7.22 (t, 1H), 7.08 (t, 1H), 6.87 (t, 1H), 6.54 (t, 1H). ¹³C NMR (DMSO-d₆, δ ppm): 173.39, 159.76, 155.83, 151.20, 150.41, 149.97, 149.55, 149.49, 147.87, 146.88, 146.57, 146.38, 137.66, 129.52, 129.40, 129.07, 126.32, 126.21, 126.16, 125.69, 125.06, 121.96, 121.14, 120.34, 119.63, 112.94, 173.39, 144.92, 144.69, 124.69, 124.48, 124.11, and 124.20.

[Ru(II)(IP)₂(Bioben)] (ClO₄)₂ (Ru-Bio): Conjugate Ru-Bio was obtained as a bright red powder. Yield: 49.3%. Anal. Calcd for C₅₅H₅₃Cl₂N₁₅O₁₁RuS (%) : C, 50.65; H, 4.10; N, 16.11. Found (%): C, 50.71; H, 4.11; N, 16.13. ESI-TOFMS (CH₃OH): m/z 1104.7496 [M-2ClO₄-H]⁺. ¹H NMR (DMSO-d₆, δ ppm): 13.48 (d, 1H), 9.03 (t, 2H), 8.97 (t, 2H), 8.72 (d, 2H), 8.64 (s, 1H), 8.55-8.46 (m, 4H), 8.33 (d, 1H), 8.13 (d, 1H), 7.92 (d, 1H), 7.79 (t, 1H), 7.73 (t, 2H), 7.65 (t, 2H), 7.57-7.34 (m, 5H), 6.43 (d, 2H), 4.48 (t, 1H), 4.41 (t, 1H), 3.64 (q, 2H), 3.44 (q, 1H), 3.39 (q, 2H), 3.21 (t, 1H), 2.98 (d, 2H), 2.42 (t, 2H), 1.99-1.79 (m, 6H), 1.73 (t, 3H), 1.63 (m, 6H). ¹³C NMR (DMSO-d₆, δ ppm): 172.33, 166.97, 164.50, 163.34, 163.19, 160.05, 159.45, 157.02, 156.08, 155.54, 154.50, 153.38, 151.64, 150.71, 149.95, 148.64, 145.03, 138.13, 137.12, 135.90, 135.03, 132.25, 131.53, 128.20, 127.67, 127.06, 124.91, 121.30, 117.08, 116.47, 61.52, 59.67, 55.91, 38.78, 35.69, 29.67, 29.63, 28.69, 28.52, 26.74, 26.65, 25.83.

[Ru(II)(PhenSe)₂(Bioben)](ClO₄)₂ (Ru-BSe): Conjugate Ru-BSe was obtained as a red powder. Yield: 37.1%. Anal. Calcd for C₅₃H₄₉Cl₂N₁₅O₁₁RuSe₂S (%) : C, 44.39; H, 3.44; N, 14.65; Found (%): C, 44.41; H, 3.56; N, 14.55. ESI-TOFMS (CH₃OH): m/z 1234.7032 [M-2ClO₄-H]⁺, 628.8790 [M-2ClO₄+Na]²⁺, 618.4017 [M-2ClO₄]²⁺. ¹H NMR (DMSO-d₆, δ ppm): 13.33 (d, 1H), 8.77 (d, 1H), 8.51 (d, 1H), 8.35 (d, 1H), 8.27 (s, 1H), 8.03 (m, 1H), 7.83 (t, 1H), 7.74 (q, 1H), 7.56 (t, 1H), 6.40 (d, 2H), 4.29 (t, 1H), 4.13 (t, 1H), 3.29 (q, 2H), 3.09 (q, 1H), 3.04 (q, 2H), 2.80 (dd, 1H), 2.57 (d, 1H), 2.08 (t, 2H), 1.65-1.40 (m, 9H), 1.40-1.20 (m, 6H). ¹³C NMR (DMSO-d₆, δ ppm): 177.58, 171.88, 168.16, 165.91, 164.69, 162.88, 161.66, 159.57, 158.14, 157.08, 156.48, 155.08, 154.62, 152.33, 142.41, 140.81, 139.29, 135.94, 134.16, 133.80, 132.97, 131.13, 130.00, 129.60, 126.54, 126.04, 117.68, 63.13, 61.21, 57.34, 36.46, 31.05, 30.22, 30.20, 29.21, 29.03, 27.20, 27.11, 26.26.

Absorption and fluorescence measurements: The spectrum of compounds were recorded under physiological condition in the PBS-DMSO solution (PBS:DMSO = 95:5, pH=7.4) at 37 °C. The UV-Vis spectrum of compounds was obtained by using a Cary 5000 UV-2450 spectrophotometer. A Shimadzu RFPC-5301 spectrofluorometer was used for recording the fluorescence spectrum.

To gain insight into the process of structural decomposition, Ru-BSe (30 μM) was incubated in 1 mM Na₂HPO₄/citric acid solution (pH=6.86) for different period of time, then both of the absorption and fluorescence spectrum were recorded. In other experiment, Ru-BSe (30 μM) was incubated in PBS-DMSO solution at different pH condition (ranging from 3.1 to 8.5) for 0 and 24 h before recording the spectrum.

Stability of Ru(II) conjugate: For ESI-TOFMS analysis, 10 mM NH₄HCO₃ solution was adjusted to pH=6.86 by adding 0.1 M HCl, and then mixed with HPLC grade MeOH at the ratio of 7:3. The decomposition process of Ru-BSe was performed as following description: Ru-BSe (10 μM) was incubated in the HPLC grade MeOH/Milli-Q H₂O solution (3:7, v:v, containing 10 mM NH₄HCO₃, pH=6.86) for 24 h at 37 °C, then 0.1 mL sample

was diluted in 1 mL HPLC grade MeOH. The diluted sample was loaded in fixed conditions and analysed by using ESI-TOFMS.

To gain more insight of the interaction between **Ru-BSe** and glutathione (GSH), the mixture was monitored by using ESI-TOFMS. The fresh prepared GSH (50 μM) and **Ru-BSe** (10 μM) were mixed in MeOH/Milli-Q H₂O solution. After the incubation at 37 °C for different period of time, 0.1 mL sample was diluted in 1 mL MeOH and loaded in fixed conditions for the ESI-TOFMS analysis.

HPLC analysis of stability of Ru-BSe in human plasma and DMSO: The plasma stability experiment was carried out according to previous studies.^[19a, 29] Diazepam (internal standard) was purchased from Sigma-Aldrich and dissolved in DMSO at the concentration of 800 μM . Stock of **Ru-BSe** and diazepam and DMSO were diluted in the human plasma solution (975 μL) to a total volume of 1000 μL , and final concentrations of 20 μM for **Ru-BSe** and 10 μM for diazepam. The resulting sample was incubated for 72 h at 37 °C with continuous and gentle shaking (ca. 300 rpm). The reaction was stopped by addition of 2 mL methanol, and the mixture was centrifuged for 45 min at 650 g at 4 °C. The methanolic solution was evaporated, and the residue was suspended in 200 μL of 1:1 (v/v) acetonitrile/H₂O. The suspension was filtered before the HPLC analysis. To examine the stability of **Ru-BSe** in DMSO, the DMSO stock solution of Ru complex (1 mM) was incubated for 72 h at 25 °C with gentle shaking (ca. 300 rpm). Afterwards, **Ru-BSe** (20 μM) was diluted in 200 μL of 1:1 (v/v) acetonitrile/H₂O before the HPLC analysis. All these samples mentioned above were analyzed by HPLC system (Agilent Technologies 1260 Infinity). The C18 reverse phase column was employed with a flow rate of 0.5 mL/min and UV-absorption was monitored at 300 nm. The runs were performed with a linear gradient of A (acetonitrile (HPLC-grade)) and B (Milli-Q water containing 0.1% trifluoroacetic acid (TFA)): t = 0–3 min, 20% A; t = 7 min, 50% A; t = 20 min, 90% A; t = 23 min, 100% A; t = 25 min, 100% A; t = 28 min, 20% A).

Cell culture and in vitro cytotoxicity evaluation: Normal human colon mucosal epithelial cell line (NCM460) was obtained from INCELL (San Antonio, TX) and maintained in INCELL's enriched M3:10 medium. The normal human liver cell line (L02) was obtained from Nanjing KeyGEN Biotech (Nanjing, China). Other human cancer cell lines, including HeLa, HepG2, MCF-7, MDA-MB-231 and A549 were obtained from American Type Culture Collection (ATCC). All cell lines were cultured in DMEM medium (except for NCM460 cells) containing 10% of the fetal bovine serum, 100 units/mL of the penicillin and 50 units/mL of the streptomycin at 37 °C in humidified incubator with 5% CO₂ atmosphere. Cell viability was determined by MTT assay that based on the capability of living cells to transform MTT to purple formazan dye. To value the anticancer potency of released therapeutic Ru complexes, the aqueous products [Ru(IP)₂Cl₂] (aq) and [Ru(phenSe)₂Cl₂] (aq) were prepared by the pre-incubation of [Ru(IP)₂Cl₂] and [Ru(phenSe)₂Cl₂] in medium at 37 °C for 12 h.

Cellular uptake of selenium compound: Briefly, 6x10⁵ HeLa cells were seeded in 6 cm dishes and supplemented with 6 mL cell culture media for 24 h. Cells were incubated with PhenSe(40 μM), **Ru-Se** (20 μM) or **Ru-BSe** (20 μM) for 2 h, and washed with PBS buffer twice. To confirm internalization via biotin receptor-mediated endocytosis, a competition assay was carried out *via* adding an excessive of biotin (100 μM) to the media. After 1 h-incubation, cells were supplied with fresh media before the treatment of selenium compounds for another 2 h and observed in fluorescent microscope. In other experiments, the intracellular concentration of Se was determined by ICP-MS analysis. After incubation of selenium compounds, cells were washed with PBS buffer twice and counted.

To investigate the mechanisms of internalization, the cellular uptake of selenium compounds was measured under different conditions.^[30] 1x10⁴ HeLa cells/well were seeded into the 96-well plates and incubated for 24 h. Cells were pretreated with sodium azide (NaN₃) 10 mM and 2-deoxy-dglucose (DOG) 50 mM, or with 100 μM biotin, or with nystatin 10 $\mu\text{g mL}^{-1}$, or with 50 mM NH₄Cl, for 1 h at 37 °C. Cells were washed with PBS buffer before incubated with 10 μM Ru(II) complexes in PBS buffer for 2 h. The effect of Ru(II) complexes diffusion into cells was examined by using hypertonic treatment. Cells were incubated with a solution of Ru(II) complexes (10 μM) and PBS solution containing 20% sucrose. After all these treatments mentioned above, cells were washed with PBS buffer for three times, followed by the lysis of cells and measure of the emission intensity at 600 nm ($\lambda_{\text{ex}} = 476 \text{ nm}$) of each well.

Determination of Ru and Se content: The samples (cells or tissues) were digested with the 3 mL acid solution (V_{HNO₃} : V_{HClO₄} = 3:1) in an infrared rapid digestion system (Gerhardt) at 180 °C for 1.5 h. The digested solution was reconstituted with Milli-Q H₂O. The Ru content in tissues was examined by ICP-AES analysis, while the intracellular Se content was tested by ICP-MS analysis.

Co-culture model for examination of selective induction of cell apoptosis: The selectivity of **Ru-BSe** between human cancer and normal cells was examined by co-culture model using TUNEL-CellTrakcer Blue co-staining assay. Briefly, 8x10⁴ L02 cells were seeded in 35-mm confocal glass dishes and allowed to attach for 24 h. Adherent L02 cells were pre-incubated with 5 μM CellTracker Blue for 1 h. After washed with PBS solution twice, L02 cells were supplied with fresh medium. Similar amount of suspended HeLa cells were cultured with adherent L02 cells for another 24 h. After treated with 20 μM of **Ru-BSe** for 24 h, the cells were fixed with 3.7% formaldehyde and permeabilized with 0.1% Triton X-100 in 10% sodium citrate solution. The fixed cells were incubated with fresh TUNEL working solution (500 μL) for 1 h at 37 °C, and observed by fluorescence microscopy.

In other experiment, after the treatment with **Ru-BSe**, the co-culture cells mentioned above were harvested before fixing with 3.7% formaldehyde. After permeabilized with 0.1% Triton X-100

solution, cells were incubated with TUNEL working solution and analyzed by flow cytometry.

Evaluation of mitochondrial membrane potential: After the treatment of Ru(II) complexes, the suspended HeLa cells were incubated in 0.5 mL JC-1 working solution at 37 °C for 10 min. Cells were centrifuged and resuspended in PBS solution before analysed by flow cytometry. The percentage of cells that lost mitochondrial membrane potential were reflected by the green fluorescence form JC-1.

Cellular localization of Ru(II) complexes: The HeLa cells were cultured in confocal dishes for 24 h before treatment of 10 μM Ru(II) complexes for 6 h, and 1 $\mu\text{g mL}^{-1}$ of DAPI and 100 nM Mito-Tracker Green for 30 min. After washing with PBS buffer twice, cell images were obtained by a fluorescence microscopy (EVOS FL auto, Life Technologies). Cells were visualized in the blue channel for DAPI ($\lambda_{\text{ex}}=345$ nm, $\lambda_{\text{em}}=430\text{--}480$ nm), the green channel for Mito-tracker ($\lambda_{\text{ex}}=488$ nm, $\lambda_{\text{em}}=500\text{--}560$ nm) and red channel for Ru complex ($\lambda_{\text{ex}}=520$ nm, $\lambda_{\text{em}}=600\text{--}650$ nm), respectively. To determine the intracellular localization of **Ru-BSe**, cell images were quantified by the software Image-Pro plus 6.0.

Determination of caspases activities: The intracellular proteins were extracted with cell lysis after the treatment of 20 μM Ru(II) complexes for 72 h. The concentration of total proteins was tested by BCA assay, and then the Caspase-3/9 activities were measured by using caspase activity kit (BD Biosciences).

Western blot analysis: The extracted proteins from Ru(II) complexes-treated HeLa cells were analyzed by Western blot according to our previous study.^[31] After separated proteins were transferred to nitrocellulose membrane, the membranes were blocked by 5% non-fat milk and incubated with primary antibodies at 4 °C overnight. Protein bands were visualized on X-ray film via the application of a chemiluminescence working solution. To confirm equal amount of proteins were loaded in each lane, β -actin was used as loading control.

Determination of ROS generation: The ROS generation in cancer cells was revealed by the increase of fluorescence intensity of DCF. Briefly, HeLa cells were seeded in 96-well plates at a density of 2×10^4 cells/well for 24 h. Cells were washed with PBS buffer twice and stained with DCFH-DA for 30 min, and then maintained in fresh PBS buffer before the treatment of Ru(II) complexes (40 μM). The fluorescence intensity of DCF (excitation/emission, 500/530 nm) was measured with fluorescence microplate reader (Tecan SAFIRE) at different time point.

Release of calcium: The content of calcium in cytoplasm was detected by Fluo 3-AM probe. 8×10^4 HeLa cells were seeded in 2 cm dishes for 24 h and then replaced by HBSS (HBSS, calcium free, magnesium free, Gibco cat. no. 14170-112). The cells were incubated with Fluo-3AM working solution in HBSS for 30 min at 37 °C and then replaced by fresh DMEM medium

containing 20 μM Ru(II) complexes. After 30-min incubation, the HeLa cells were observed using a fluorescence microscopy.

Mouse xenograft model: About 1×10^6 cells were subcutaneously injected in the left leg of BALB/c nude mice to construct the HeLa xenograft model. When the tumor volume reach upon 100 mm^3 , the tumor-bearing mice were randomly divided in 5 groups (n=6 each group). To examine the therapeutic effect of Se-containing complexes, the HeLa xenograft models were respectively received tail intravenous injection treatment of 2 $\mu\text{mol/kg}$ or 4 $\mu\text{mol/kg}$ **Ru-Se**, 2 $\mu\text{mol/kg}$ or 4 $\mu\text{mol/kg}$ **Ru-BSe** per 2 days for 30 days treatment. The control group mice were injected with equal amount of saline. The maximal length (l) and the width (w) of the tumor were measured for the calculation of tumor volume by following the equation: Volume (mm^3) = $lw^2/2$. At the end of treatment, the tumor and the normal organs were obtained for histological analysis and determination of Ru content. To detect the apoptotic cells in tumor, the TUNEL staining assay was carried out.

In vivo and ex vivo fluorescence imaging: To evaluate the theranostic effect of Ru(II) complexes, 4 $\mu\text{mol/kg}$ of complexes in 0.2 mL of 0.9% NaCl solution was injected into the tail-vein of HeLa xenografts nude mice. Afterwards, the mice were anesthetized and monitored with fluorescence imaging system (Night OWL II LB 983) at different time points (0, 24, 48 and 72 h). After 72 h treatment, the brain, heart, liver, spleen, lungs, kidney and tumor of each group were collected for the determination of biodistribution of Ru complexes by using fluorescence imaging technique. Fluorescent filter sets are used for *in vivo* and *ex vivo* fluorescent imaging (excitation/emission, 500/640 nm), which are similar with previous studies.^[3]

Hematology analysis of nude mice: After the treatment of Ru(II) complexes, the blood samples were collected from normal and xenograft mice. The plasma was obtained by centrifuging blood samples at 3,000 rpm for 10 min and then subjected to hematology analysis. The tested biochemical indexes included uric acid (UA), blood urea nitrogen (BUN), creatinine (CREA), triglyceride (TG), aminotransferase (AST), total protein (TP), albumin (ALB) and creatine kinase (CK).

Acknowledgements

Acknowledgements Text. This work was supported by National High-level Personnel of Special Support Program (2014189), YangFan Innovative & Entrepreneurial Research Team Project (201312H05), Guangdong Special Support Program and Fundamental Research Funds for the Central Universities.

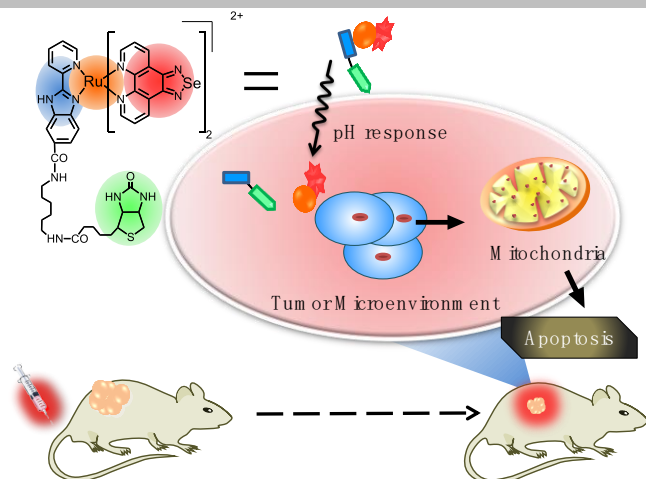
Keywords: selenium • theranosis • tumor microenvironment-responsive • cancer targeting.

- [1] C. Liang, L. Xu, G. Song, Z. Liu, *Chem. Soc. Rev.* **2016**, *45*, 6250-6269.
- [2] R. Kumar, W. S. Shin, K. Sunwoo, W. Y. Kim, S. Koo, S. Bhuniya, J. S. Kim, *Chem. Soc. Rev.* **2015**, *44*, 6670-6683.
- [3] a) R. Kumar, J. Han, H. J. Lim, W. X. Ren, J. Y. Lim, J. H. Kim, J. S. Kim, *J. Am. Chem. Soc.* **2014**, *136*, 17836-17843; b) X. Wu, X. Sun, Z. Guo, J. Tang, Y. Shen, T. D. James, H. Tian, W. Zhu, *J. Am. Chem. Soc.* **2014**, *136*, 3579-3588.
- [4] a) M. Ye, X. Wang, J. Tang, Z. Guo, Y. Shen, H. Tian, W. H. Zhu, *Chem. Sci.* **2016**, *7*, 4958-4965; b) J. Z. Du, X. J. Du, C. Q. Mao, J. Wang, *J. Am. Chem. Soc.* **2011**, *133*, 17560-17563.
- [5] a) Q. Zhao, C. H. Huang, F. Y. Li, *Chem. Soc. Rev.* **2011**, *40*, 2508-2524; b) L. He, C. P. Tan, R. R. Ye, Y. Z. Zhao, Y. H. Liu, Q. Zhao, L. N. Ji, Z. W. Mao, *Angew. Chem. Int. Ed.* **2014**, *53*, 12137-12141.
- [6] L. Zeng, P. Gupta, Y. Chen, E. Wang, L. Ji, H. Chao, Z. S. Chen, *Chem. Soc. Rev.* **2017**, *46*, 5771-5804.
- [7] D. L. Ma, H. Z. He, K. H. Leung, D. S. H. Chan, C. H. Leung, *Angew. Chem. Int. Ed.* **2013**, *52*, 7666-7682.
- [8] a) S. Imstepf, V. Pierroz, R. Rubbiani, M. Felber, T. Fox, G. Gasser, R. Alberto, *Angew. Chem. Int. Ed.* **2016**, *55*, 2792-2795; b) R. R. Ye, C. P. Tan, L. He, M. H. Chen, L. N. Ji, Z. W. Mao, *Chem. Commun.* **2014**, *50*, 10945-10948.
- [9] P. D. Hanavan, C. R. Borges, B. A. Katchman, D. O. Faigel, T. H. Ho, C. T. Ma, E. A. Sergienko, N. Meurice, J. L. Petit, D. F. Lake, *Oncotarget* **2015**, *6*, 18418-18428.
- [10] Y. Liu, Y. Luo, X. Li, W. Zheng, T. Chen, *Chem. Asian J.* **2015**, *10*, 642-652.
- [11] Y. Chen, L. Qiao, L. Ji, H. Chao, *Biomaterials* **2014**, *35*, 2-13.
- [12] a) Z. Deng, L. Yu, W. Cao, W. Zheng, T. Chen, *Chem. Commun.* **2015**, *51*, 2637-2640; b) L. He, T. Chen, Y. You, H. Hu, W. Zheng, W. L. Kwong, T. T. Zou, C. M. Che, *Angew. Chem. Int. Ed.* **2014**, *53*, 12532-12536.
- [13] a) L. Murphy, A. Congreve, L. O. Palsson, J. A. G. Williams, *Chem. Commun.* **2010**, *46*, 8743-8745; b) L. He, Y. Li, C. P. Tan, R. R. Ye, M. H. Chen, J. J. Cao, L. N. Ji, Z. W. Mao, *Chem. Sci.* **2015**, *6*, 5409-5418.
- [14] W. C. Huang, S. H. Chen, W. H. Chiang, C. W. Huang, C. L. Lo, C. S. Chern, H. C. Chiu, *Biomacromolecules* **2016**, *17*, 3883-3892.
- [15] C. J. Cheng, R. Bahal, I. A. Babar, Z. Pincus, F. Barrera, C. Liu, A. Svoronos, D. T. Braddock, P. M. Glazer, D. M. Engelman, W. M. Saltzman, F. J. Slack, *Nature* **2015**, *518*, 107-110.
- [16] a) Y. Z. Min, C. Q. Mao, S. M. Chen, G. L. Ma, J. Wang, Y. Z. Liu, *Angew. Chem. Int. Ed.* **2012**, *51*, 6742-6747; b) T. T. Zou, C. T. Lum, S. S. Y. Chui, C. M. Che, *Angew. Chem. Int. Ed.* **2013**, *52*, 2930-2933.
- [17] a) S. J. Dougan, A. Habtemariam, S. E. McHale, S. Parsons, P. J. Sadler, *Proc. Natl. Acad. Sci. USA* **2008**, *105*, 11628-11633; b) T. Zou, C. T. Lum, C. N. Lok, W. P. To, K. H. Low, C. M. Che, *Angew. Chem. Int. Ed.* **2014**, *53*, 5810-5814.
- [18] a) M. Li, J. W. Y. Lam, F. Mahtab, S. J. Chen, W. J. Zhang, Y. N. Hong, J. Xiong, Q. C. Zheng, B. Z. Tang, *J. Mater. Chem. B* **2013**, *1*, 676-684; b) S. Bhuniya, S. Maiti, E. J. Kim, H. Lee, J. L. Sessler, K. S. Hong, J. S. Kim, *Angew. Chem. Int. Ed.* **2014**, *53*, 4469-4474.
- [19] a) V. Pierroz, T. Joshi, A. Leonidova, C. Mari, J. Schur, I. Ott, L. Spiccia, S. Ferrari, G. Gasser, *J. Am. Chem. Soc.* **2012**, *134*, 20376-20387; b) R. A. Smith, C. M. Porteous, A. M. Gane, M. P. Murphy, *Proc. Natl. Acad. Sci. U.S.A.* **2003**, *100*, 5407-5412; c) W. Lv, Z. Zhang, K. Y. Zhang, H. R. Yang, S. J. Liu, A. Q. Xu, S. Guo, Q. Zhao, W. Huang, *Angew. Chem. Int. Ed.* **2016**, *55*, 9947-9951.
- [20] J. Chen, Z. Luo, Z. Zhao, L. Xie, W. Zheng, T. Chen, *Biomaterials* **2015**, *71*, 168-177.
- [21] L. Xie, Z. Luo, Z. Zhao, T. Chen, *J. Med. Chem.* **2017**, *60*, 202-214.
- [22] S. Cory, J. M. Adams, *Nat. Rev. Cancer* **2002**, *2*, 647-656.
- [23] A. Martin, A. Byrne, C. S. Burke, R. J. Forster, T. E. Keyes, *J. Am. Chem. Soc.* **2014**, *136*, 15300-15309.
- [24] a) Y. M. Ma, Y. M. Peng, Q. H. Zhu, A. H. Gao, B. Chao, Q. J. He, J. Li, Y. H. Hu, Y. B. Zhou, *Acta Pharmacol. Sin.* **2016**, *37*, 1381-1390; b) W. Chen, P. Zou, Z. Zhao, Q. Weng, X. Chen, S. Ying, Q. Ye, Z. Wang, J. Ji, G. Liang, *Oncotarget* **2016**, *7*, 16593-16609.
- [25] R. Cao, J. Jia, X. Ma, M. Zhou, H. Fei, *J. Med. Chem.* **2013**, *56*, 3636-3644.
- [26] R. Schiffmann, A. Neugebauer, C. D. Klein, *J. Med. Chem.* **2006**, *49*, 511-522.
- [27] R. Kottani, R. A. Valiulin, A. G. Kutateladze, *Proc. Natl. Acad. Sci. U.S.A.* **2006**, *103*, 13917-13921.
- [28] C. A. Puckett, J. K. Barton, *J. Am. Chem. Soc.* **2007**, *129*, 46-47.
- [29] H. Y. Huang, B. L. Yu, P. Y. Zhang, J. J. Huang, Y. Chen, G. Gasser, L. N. Ji, H. Chao, *Angew. Chem. Int. Ed.* **2015**, *54*, 14049-14052.
- [30] Z. N. Zhao, Z. D. Luo, Q. Wu, W. J. Zheng, Y. X. Feng, T. F. Chen, *Dalton Trans.* **2014**, *43*, 17017-17028.
- [31] Y. Huang, L. He, W. Liu, C. Fan, W. Zheng, Y.-S. Wong, T. Chen, *Biomaterials* **2013**, *34*, 7106-7116.

Entry for the Table of Contents

Layout 2:

FULL PAPER



Zhennan Zhao, Pan Gao, Yuanyuan You and Tianfeng Chen*

Page No. – Page No.

Cancer-targeting Functionalization of Selenium-containing Ruthenium Conjugate with Tumor Microenvironment- Responsive Property to Enhance Theranostic Effects

Herein we demonstrate the rational design and synthesis of a selenium-containing conjugate that could selectively recognize cancer cells to realize enhanced theranostic effects and nullify the systemic toxicity. The protonation process of Ru(II) conjugate in tumor acidic microenvironment cause ligand substitution, resulting in release of activated metallodrug that trigger apoptosis in tumor tissue.